

## **LOW TEMPERATURE SPECIFIC HEAT CAPACITY OF 3d TRANSITION METAL CHLORINE BORACITES ( $T_3B_7O_{13}Cl$ ; $T=Cr, Mn, Fe, Co, Ni, Cu, Zn$ or $Mg$ )**

*W. Schnelle<sup>1\*</sup>, E. Gmelin<sup>1</sup>, O. Crottaz<sup>2</sup> and H. Schmid<sup>2</sup>*

<sup>1</sup>Max-Planck-Institut für Festkörperforschung, Heisenbergstr. 1, D-70569 Stuttgart, Germany

<sup>2</sup>Université de Genève, Dept. de Chimie Minérale, Analytique et Appliquée, 30 Quai Ernest-Ansermet, CH-1211 Genève 4, Switzerland

### **Abstract**

The heat capacities of eight chlorine boracites  $T_3B_7O_{13}Cl$  ( $T=Cr, Mn, Fe, Co, Ni, Cu, Zn$  or  $Mg$ ) have been measured in the temperature range 2 to 100 K. Magnetic phase transitions occur below 20 K in the compounds studied except in the two non-magnetic substances  $Zn_3B_7O_{13}Cl$  and  $Mg_3B_7O_{13}Cl$ . The magnetic specific heat capacities give information on magnetic ground state of the transition metals and the entropy related to the phase transitions.

**Keywords:** magnetic phase transition, specific heat capacity, transition metal compound

### **Introduction**

The compounds which belong to the crystal family known as boracites have the general formula  $T_3B_7O_{13}X$ , where  $T$  stands for a bivalent metal cation ( $Mg, Cr, Mn, Fe, Co, Ni, Cu, Zn$  and  $Cd$ ) and  $X$  for a monovalent anion ( $OH, F, Cl, Br, I, NO_3$ ). The compounds comprise today a great variety of synthetic homologues derived from the crystal structure of the mineral boracite,  $Mg_3B_7O_{13}Cl$  [1–4]. They attracted particular interest due to the occurrence of simultaneous ferroelectricity/ferroelasticity and (weak) ferromagnetism in  $Ni_3B_7O_{13}I$  [3, 5]. Nearly all  $T-X$  boracites are characterised by a sequence of structural phase transitions from a high-temperature cubic phase to orthorhombic or rhombohedral ferroelectric/ferroelastic phases which order magnetically at low temperatures. Triangular geometric magnetic frustration exists in all non-cubic boracites. Whereas the ferroelectric/ferroelastic phase transition above room temperature of some of the boracites has been characterised thermodynamically, no low temperature heat capacity data, with exception of  $Co_3B_7O_{13}X$  ( $X=Cl, Br, I$ ) [6], exist for the boracites.

The present paper reports on the low temperature specific heats and entropy values related to the magnetic phase transitions in the chlorine boracites ( $T=Cr, Mn, Fe, Co, Ni, Cu$  and  $Zn, Mg$  with  $X=Cl$ ) in the temperature range between 2 and 100 K.

\* Present address: Max Planck-Institut für Chemische Physik fester Stoffe, Pirnaer Landstr. 176, D-01257 Dresden, Germany

The data complement earlier magnetic susceptibility, dielectric permittivity, electrical polarisation, magnetic birefringence and magnetoelectric measurements [3, 5, 7–9].

## Experimental

The single crystalline or polycrystalline samples were grown by chemical transport reaction as described in Ref. [10]. Either an automated quasi-adiabatic calorimeter [11] or a low temperature scanning calorimeter [12], using sample masses between 170 and 570 mg, served to determine the heat capacity. The inaccuracy is estimated to be <2% below 30 K for the magnetic compounds and increases to  $\approx 5\%$  for some of the samples near 100 K.

## Results and discussion

The molar heat capacity  $c_p(T)$  of the chlorine boracites is shown in Fig. 1. With exception of the two non-magnetic compounds  $Zn_3B_7O_{13}Cl$  and  $Mg_3B_7O_{13}Cl$ , the compounds display magnetic ordering below about 20 K. Near 60 K all  $c_p(T)$  data merge together as expected for the pure lattice heat of isomorphous compounds with nearly identical molar masses and lattice constants.  $Mg_3B_7O_{13}Cl$ , however, shows a significantly lower  $c_p(T)$  as a result of the much lower molar mass. It is given here only for comparison. At higher temperatures the lattice heats deviate from a common curve due to differences of the elastic constants and masses or simply because of errors resulting from the small sample masses available. The non magnetic Zn–Cl boracite serves as reference for the lattice heat of other compounds. Due to the low mass of constituting atoms, the Debye temperatures  $\Theta$  of the boracites are high and thus the lattice contribution is rather small. The equivalent Debye temperature of  $Zn_3B_7O_{13}Cl$  between 30 and 100 K ranges from  $\Theta=510$  to  $\Theta=700$  K. The magnetic specific heat  $c_{mag}(T)$  was calculated as the difference between the measured total and the lattice heat (of Zn–Cl boracite) for each compound.  $c_{mag}(T)$  is shown in Fig. 2 as

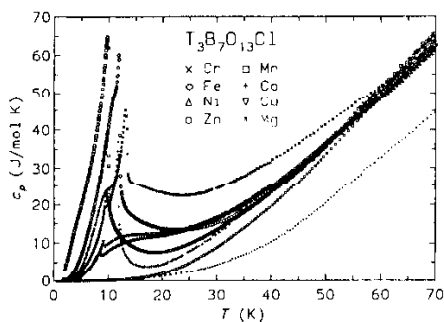


**Fig. 1** Temperature dependence of the molar heat capacities of chlorine boracites,  $T_3B_7O_{13}Cl$  ( $T=Cr, Mn, Fe, Co, Ni,$  and  $Cu$ ) and of the non-magnetic compounds  $Zn_3B_7O_{13}Cl$  and  $Mg_3B_7O_{13}Cl$  as reference material for the lattice heat capacity

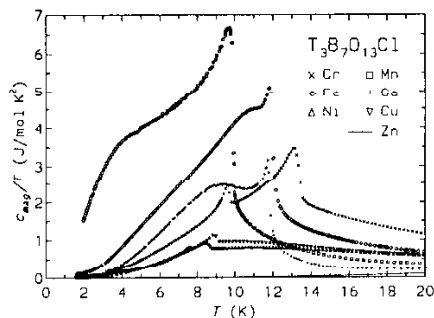


Fig. 2 Magnetic specific heat  $c_{\text{mag}}/T$  vs.  $T$  of the compounds shown in Fig. 1

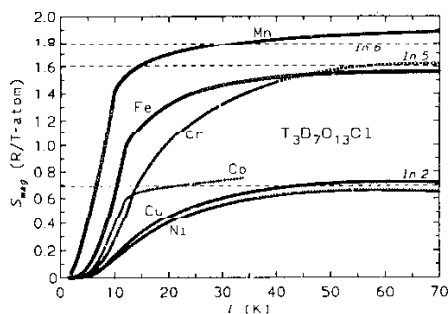


Fig. 3 Magnetic entropies  $S_{\text{mag}}(T)$  calculated from the magnetic part of the specific heat, derived from Figs 1 and 2

a plot  $c_{\text{mag}}/T$  vs.  $T$ . Integration yields the magnetic entropy contributions  $S_{\text{mag}}$  ( $S = \int [c_{\text{mag}}(T)/T]dT$ ) which gives information on the degeneracy of the 3d ions and the number of spins involved in the magnetic transition. The magnetic entropies per  $T$ -atom are plotted in Fig. 3 as a function of temperature. Some characteristic values related to the magnetic ordering, as magnetic ordering temperature, related entropy, and spin ground state of the  $T^{2+}$  ions are listed in Table 1.

According to the shape of the transition peaks, shown in Figs 1 and 2, different types of magnetic ordering occur in the chlorine boracite series.

### $Mn_3B_7O_{13}Cl$

The orthorhombic compound (space group:  $Pca2_1'$ ; point group notation:  $mm2'$ ) displays a sharp lambda-type transition at 11 K, which is typical for three-dimensional (3D) ordering. At  $T_N$  the compound transforms into a weakly ferromagnetic phase and the transition displays second order character in the magnetisation curves [13]. For the Mn-Cl boracite the magnetic symmetry and structure below  $T_N$  has not yet been determined, however, the magnetic and magneto-elastic properties

**Table 1** Characteristic values of magnetic ordering of chlorine boracites  $T_3B_7O_{13}Cl$  ( $T=$  3d-transition metals) at low temperatures

Chlorine boracites $T$	Magnetic ordering $T_N/K$	Ground state $S$	Entropy $S(th)/$ $J(mol\ K)^{-1}$	Entropy $S(ex)/S(th)/$ %	Entropy $S(T_N)/S(th)/$ %
Cr	13.2	2	$R\ln 5$	98	38
Mn	9.8	$5/2$	$R\ln 6$	106	79
Fe	11.8	2	$R\ln 5$	95	59
Co	11.7	$3/2$	$R\ln 4$	100 of $R\ln 2$	81
Ni	8.5	1	$R\ln 3$	100 of $R\ln 2$	13
Cu	9.0	$1/2$	$R\ln 2$	102	18

The saturation values of the magnetic entropy  $S_{mag}$  are denoted in the table as following:  $S(th)$  – expected theoretically taking  $S_{mag}=R(2S+1)$ ,  $S(ex)$  – experimentally found as saturation value, and  $S(T_N)$  – the value reached at the ordering temperature  $T_N$ ,  $R$  – value of gas constant

are expected to be similar to Mn I, i.e. transition from  $Pca2_1'$  into  $Pc'a2_1'$  [14]. The entropy indicates the usual ground state for all three  $Mn^{2+}$  ions with spin  $S=5/2$ , yielding a high-temperature limiting entropy value of  $S_{mag}=3R\ln(2S+1)=3R\ln 6$  ( $R$ =gas constant). Thus, magnetic and thermal data are consistent.

### $Fe_3B_7O_{13}Cl$ and $Co_3B_7O_{13}Cl$

$Fe_3B_7O_{13}Cl$  and  $Co_3B_7O_{13}Cl$ , show shoulders at the low temperature flank of the sharp peak at the Néel point at 11.8 and 11.5 K, respectively. In contrast to  $Mn_3B_7O_{13}Cl$ , the paramagnetic rhombohedral ( $R3c1'$ ) ferroelectric/ferroelastic phase undergoes a spin ordering to a monoclinic ( $Cc$ ), fully ferroelectric/ferroelastic and partially weakly ferromagnetic structure [15]. For the Co–Cl compound, the magnetic phase has recently been determined at 1.5 K using neutron scattering [16]. In the compounds Co–Br and Co–I, however, the weak shoulder found in Co–Cl appears not only as a shoulder but as a clear additional phase transitions in the specific heat near  $T_N/2$ . This behaviour hints to a continuous spin reorientation which was confirmed by the spin structure determined using neutron scattering experiments on the Co–Br compound where the spin-structure transforms at lowering the temperature to a canted 3D structure [17]. The continuous spin reorientation may thermodynamically be represented by a two-level system which leads to a Schottky-type anomaly in the specific heat which may be the origin of the weak shoulder in the specific heat of Co–Cl. The findings of the heat capacity measurements, i.e. the sharp ordering and the spin reorientation, are for both compounds in agreement with the other experimental results, e.g. spontaneous polarisation, magneto-electric measurements, etc. [18]. The entropy curve indicates for Fe–Cl the expected  $Fe^{2+}$  ( $S=2$ ) ground state (yielding  $S=R\ln 5$ ) whereas due to a large spin-orbit coupling the magnetic ground state of Co–Cl is a doublet and the ion is an effective spin  $1/2$  system near  $T_N$ , giving an average entropy value of  $S=R\ln 2$  per Co-atom.

### *Cr<sub>3</sub>B<sub>7</sub>O<sub>13</sub>Cl*

In Cr–Cl boracite two magnetic transitions are observed in the specific heat. The orthorhombic phase (Pca2<sub>1</sub>' ) undergoes a transition at 13.5 K (Néel point) to an antiferromagnetic ferroelectric/ferroelastic phase which transforms again into a weakly ferromagnetic system at 9.7 K. Both transitions have been observed earlier by magnetoelectric experiments and in the spontaneous polarisation [19]. The magnetic heat capacity above the transition is unusually high (Fig. 2). The greater part of the magnetic entropy is engaged in short range ordering above  $T_N$ , i.e. more than 50% according to Fig. 3. This finding hints to a tendency for lower than three-dimensional ordering in the Cr–Cl compound or stronger geometric frustration. The chromium occupies in this compound the usual  $\text{Cr}^{2+}$  ( $S=2$ ) ground state and thus  $S=3R\ln 5$ .

### *Cu<sub>3</sub>B<sub>7</sub>O<sub>13</sub>Cl and Ni<sub>3</sub>B<sub>7</sub>O<sub>13</sub>Cl*

Both compounds have a structure isostructural to Mn–Cl. Magnetic ordering has been detected previously by several techniques [20, 21], in particular by neutron scattering for Ni–Cl [22]. However, the specific heat results do not show a sharp transition (Fig. 2). The 'smooth' transitions hint to short range spin ordering in a low dimension, according to the neutron scattering results along the 180°  $\text{Ni}^{2+}$ –Cl– $\text{Ni}^{2+}$  path and frustrated due to the 90°  $\text{Ni}^{2+}$ –Cl– $\text{Ni}^{2+}$  path with competing ferromagnetic interactions. Presumably, the Cu–Cl boracite behaves similar. The related entropies indicate a spin 1/2 ground state ( $S=R\ln 2$ ) for both compounds although for  $\text{Ni}^{2+}$   $S=1$  is expected. However, it is also possible that in Ni–Cl boracite only two of the three  $\text{Ni}^{2+}$  ions participate in the ordering while  $2R\ln 3 \approx 3R\ln 2$ .

## Conclusions

Summarising, the specific heat capacity of chlorine boracites display sharp magnetic ordering transitions for the Mn, Fe and Co compounds whereas the Cr–Cl compounds shows a pronounced short range ordering tail indicating either magnetic frustration or low dimensional magnetic ordering. Specific heat curves, typical for low dimensional magnetic ordering, are found for the Cu–Cl and Ni–Cl boracites. The results of the heat capacity measurements are consistent with the earlier reported data for magnetic susceptibility, dielectric permittivity, electrical polarisation, magnetic birefringence, magnetoelectric measurements and neutron scattering. More detailed work on the magnetic structure of the materials is clearly needed.

## References

- 1 H. Schmid, *Ferroelectrics*, 162 (1994) 317.
- 2 J.-P. Rivera, *Ferroelectrics*, 161 (1994) 165.
- 3 J.-P. Rivera and H. Schmid, *Ferroelectrics*, 36 (1981) 447.
- 4 H. Schmid, *Phys. stat. sol.*, 37 (1970) 209.
- 5 E. Ascher, H. Rieder, H. Schmid and H. Stössel, *J. Appl. Phys.*, 37 (1966) 1404.

- 6 M. Clin, W. Dai, E. Gmelin and H. Schmid, *Ferroelectrics*, 108 (1990) 201.
- 7 H. Schmid, H. Rieder and E. Ascher, *Solid State Commun.*, 3 (1965) 327.
- 8 P. Tolédamo, H. Schmid, M. Clin and J.-P. Rivera, *Phys. Rev.*, B 32 (1985) 6006.
- 9 M. Clin, J.-P. Rivera and H. Schmid, *Ferroelectrics*, 108 (1990) 207.
- 10 H. Schmid and H. Tippmann, *J. Crystal Growth*, 46 (1979) 723.
- 11 E. Gmelin, *Thermochim. Acta*, 92 (1985) 53.
- 12 W. Schnelle and E. Gmelin, *Thermochim. Acta*, 269/270 (1995) 27.
- 13 O. Crottaz, P. Schobinger-Papamantellos, E. Suard, C. Ritter, S. Gentil, J.-P. Rivera and H. Schmid, *Ferroelectrics*, 204 (1997) 45.
- 14 O. Crottaz, J.-P. Rivera, B. Revaz and H. Schmid, *Ferroelectrics*, 204 (1997) 125.
- 15 H. Schmid, *Ferroelectrics*, 162 (1994) 317.
- 16 P. Schobinger-Papamantellos, Z.-G. Ye, H. Schmid, C. Ritter and E. Suard, 3rd Int. Conf. on Magnetoelectric Interaction Phenomena in Crystals (MEIPIC-3), Novgorod 1996, to be published.
- 17 P. Schobinger-Papamantellos, P. Fischer, F. Kubel and H. Schmid, *Ferroelectrics*, 162 (1994) 93.
- 18 M. Senthil Kumar, J.-P. Rivera, Z.-G. Ye, D. Gentil and H. Schmid, *Ferroelectrics*, 204 (1997) 57, and refs therein.
- 19 J.-P. Rivera, *Ferroelectrics*, 161 (1994) 165.
- 20 J.-P. Rivera and H. Schmid, *J. Physique Colloque C8, Suppl. 12*, 49 (1988) 849.
- 21 J.-P. Rivera and H. Schmid, *J. Appl. Phys.*, 70 (1991) 6410, and refs therein.
- 22 Z.-G. Ye, P. Schobinger-Papamantellos, S.-Y. Mao, C. Ritter, E. Suard, M. Sato and H. Schmid, *Ferroelectrics*, 204 (1997) 83.